

RESEARCH ARTICLE

FilGAP, a Rho–ROCK-regulated GAP for Rac, controls adherens junctions in MDCK cells

Shinichiro Nakahara*, Koji Tsutsumi*, Takuya Zuinen and Yasutaka Ohta[†]

ABSTRACT

Rho family small GTPases are essential for the formation of adherens junctions in epithelial cells. Here, we found that FilGAP (also known as ARHGAP24), a Rac-specific Rho GTPase-activating protein, promoted the formation of adherens junctions in Madin–Darby canine kidney (MDCK) cells. Knockdown of FilGAP by siRNA stimulated the disassembly and migration of MDCK cells induced by hepatocyte growth factor (HGF). By contrast, forced expression of FilGAP induced accumulation of E-cadherin at adherens junctions. Endogenous FilGAP colocalized with E-cadherin at adherens junctions, and depletion of FilGAP reduced the amount of E-cadherin expressed at the surface. The Rac GAP domain of FilGAP was necessary for the suppression of cell scattering induced by HGF. In agreement with this, siRNA-mediated knockdown of both Rac1 and FilGAP suppressed cell scattering induced by HGF. Forced expression of Rho kinase (ROCK, of which there are two isoforms ROCK1 and ROCK2) induced the accumulation of E-cadherin at the adherens junction, and depletion of FilGAP prevented the accumulation of E-cadherin. Moreover, wild-type FilGAP but not a non-phosphorylatable FilGAP mutant rescued the accumulation of E-cadherin at adherens junctions. These results suggest that FilGAP might regulate cell–cell adhesion through inactivation of Rac downstream of Rho–ROCK-signaling in MDCK cells.

KEY WORDS: Rac, Rho, Adherens junctions, E-cadherin, EMT

INTRODUCTION

Cell–cell adhesion is essential for epithelial tissue integrity and function. Adherens junctions are responsible for epithelial cell–cell adhesions and are composed of a transmembrane protein E-cadherin that is connected to actin cytoskeleton through catenins (Green et al., 2010). Several lines of evidence indicate that the actin cytoskeleton and its regulators are crucially involved in the regulation of E-cadherin functions (Briehner and Yap, 2013; Niessen et al., 2011).

Rho family small GTPases (Rho GTPases) regulate many fundamental cellular processes including cell adhesion, migration, vesicle trafficking and differentiation (Heasman and Ridley, 2008; Jaffe and Hall, 2005; Parsons et al., 2010). The GTP-bound active form stimulates downstream effectors, whereas hydrolysis of GTP inactivates Rho GTPases. Therefore, these proteins cycle between an inactive GDP-bound state and an active GTP-bound state. Two classes of proteins mainly regulate this cycle. Guanine-nucleotide-exchange factors (GEFs) activate Rho GTPase by catalyzing the

exchange of GDP for GTP, whereas GTPase-activating proteins (GAPs) stimulate the intrinsic GTPase activity and inactivate them (Bos et al., 2007). Because Rho GTPases are involved in the control of actin cytoskeleton, they play an important role in the regulation of E-cadherin-mediated cell–cell adhesion (McCormack et al., 2013).

Cell–cell adhesion is regulated spatiotemporally by Rho GTPases. Rac is activated as an early response to E-cadherin ligation (Ehrlich et al., 2002; Kovacs et al., 2002; Noren et al., 2001). Initial activation of Rac induces inactivation of RhoA through activation of p190RhoGAP (also known as ARHGAP35) and Rac activity is gradually replaced by RhoA, which is mainly responsible for adhesion strength and the maturation of adherens junctions (Guilluy et al., 2011; Noren et al., 2003; Yamada and Nelson, 2007). The requirement of RhoA signaling for cell–cell adhesion is mediated by actin-binding proteins and myosin (Niessen et al., 2011). It has been shown that a number of Rho GEFs and Rho GAPs are involved in the control of spatial regulation of Rho GTPases (Ngok et al., 2014; Niessen et al., 2011). However, it is largely unclear how RhoA and Rac are spatially segregated at cell–cell junctions.

FilGAP (also known as ARHGAP24) is a Rac-specific GAP that suppresses Rac-dependent lamellipodia formation and cell spreading (Nakamura, 2013; Ohta et al., 2006). FilGAP is phosphorylated by ROCK, and this phosphorylation stimulates its RacGAP activity (Ohta et al., 2006). Depletion of endogenous FilGAP induces a Rac-driven elongated mesenchymal morphology. By contrast, overexpression of FilGAP induces membrane blebbing and a rounded amoeboid morphology in a manner that requires Rho–ROCK-dependent phosphorylation of FilGAP (Saito et al., 2012). Thus, FilGAP mediates the antagonism of Rac by Rho that suppresses a mesenchymal morphology and promotes amoeboid migration (Guilluy et al., 2011; Nakamura, 2013; Saito et al., 2012).

Hepatocyte growth factor (HGF) stimulates disruption of cell–cell junctions and enhances cell migration and scattering in epithelial cell lines including MDCK cells (Kodama et al., 2000). The HGF receptor Met is often overexpressed or mutated in cancers (Graveel et al., 2013). However, it is not clear how Met signaling mediates diverse cellular responses such as motility, invasion and growth.

In this study, we demonstrate that FilGAP acts downstream of Rho–ROCK to specifically inactivate Rac at adherens junctions. We found that forced expression of FilGAP suppressed HGF-induced cell scattering. Hence, FilGAP might stabilize cell–cell adhesion through inactivation of Rac in MDCKII cells.

RESULTS

FilGAP suppresses HGF-mediated cell scattering

To study the role of FilGAP in the maintenance of adherens junctions, MDCKII cells were transfected with FilGAP siRNA for 48 h. siRNAs targeting FilGAP effectively reduced the expression of endogenous FilGAP in MDCKII cells (Fig. 1B). Depletion of

Division of Cell Biology, Department of Biosciences, School of Science, Kitasato University, Kanagawa 252-0373, Japan.

*These authors contributed equally to this work

[†]Author for correspondence (yohta@kitasato-u.ac.jp)

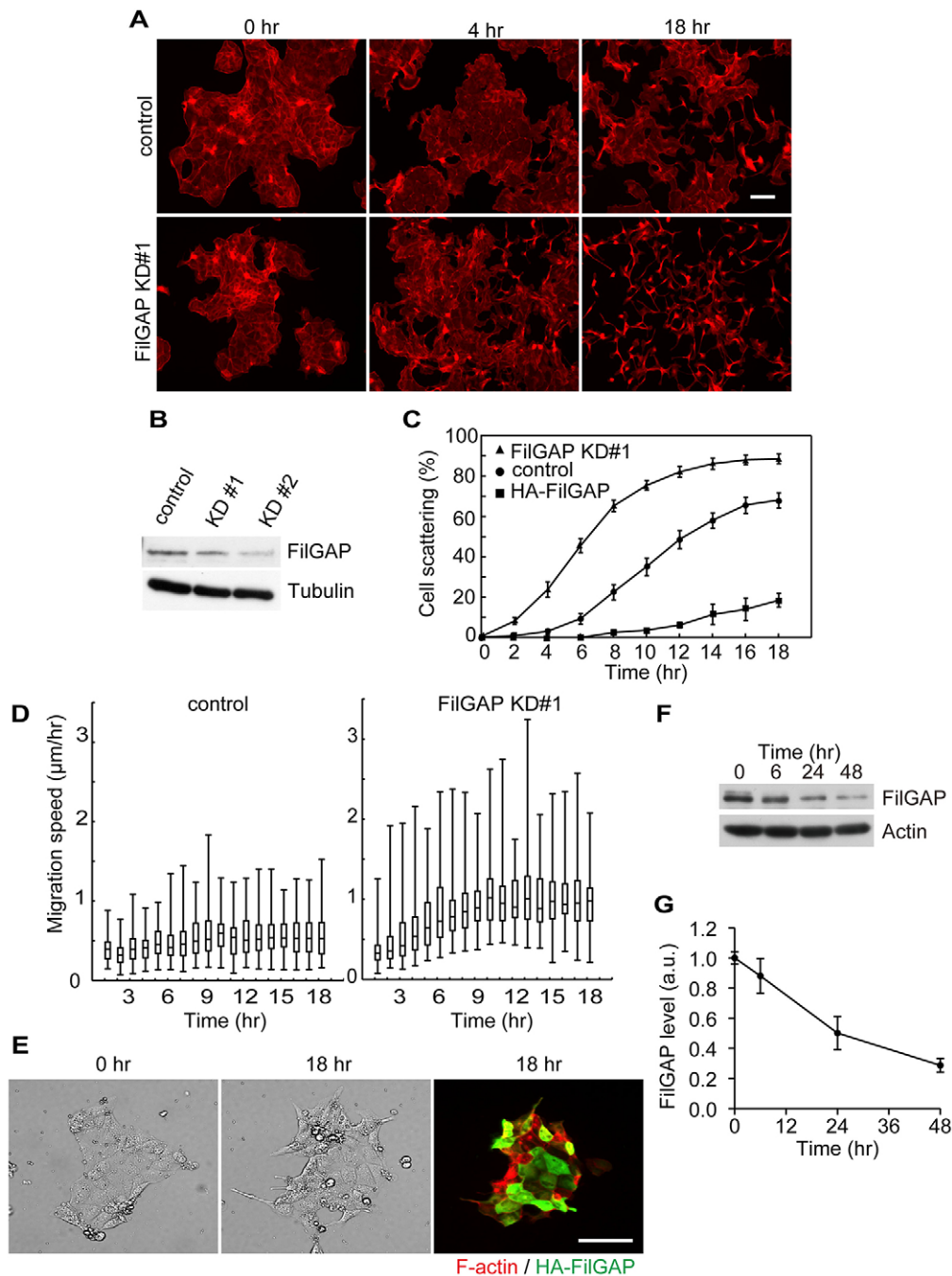


Fig. 1. FilGAP regulates cell–cell junction formation and inhibits HGF-mediated scattering.

(A) MDCKII cells were transfected with control or FilGAP siRNA for 2 days. Then the cells were fixed 4 or 18 h after the treatment with HGF (20 ng/ml). F-actin was stained with Alexa-Fluor-568-labeled phalloidin. Scale bar: 100 μm . (B) Immunoblot showing that FilGAP is depleted after 2 days of siRNA treatment (KD #1, KD #2) in MDCKII cells. Tubulin was used as a loading control. (C) The percentages of scattering cells after treatment with HGF were calculated. Data are expressed as the mean \pm s.e.m. ($n=3$). (D) MDCKII cells transfected with control or FilGAP siRNA were treated with HGF (20 ng/ml) and monitored by time-lapse phase-contrast microscopy for 18 h. The velocities of migrating cells were calculated every hour and the data are expressed as box plots. The box represents the 25–75th percentiles, and the median is indicated. The whiskers show the highest and lowest values. (E) MDCKII cells were transiently transfected with HA-tagged FilGAP. After 24 h, the cells were treated with HGF (20 ng/ml) and visualized by time-lapse phase-contrast microscopy for 18 h. After recording, the cells were fixed and stained with anti-HA antibody for HA-FilGAP (green) and Alexa-Fluor-568-labeled phalloidin for F-actin (red). Images at the 0 and 18 h time points are shown. Scale bar: 100 μm . (F) Immunoblot showing that expression of FilGAP decreases after treatment of the cells with HGF (20 ng/ml). Actin was used as a loading control. (G) Quantitative analysis of expression of FilGAP protein after treatment with HGF (20 ng/ml). The data are expressed as the mean \pm s.e.m. ($n=3$).

endogenous FilGAP by siRNA alone did not induce cell–cell detachment (Fig. 1A,C). However, knockdown of FilGAP stimulated HGF-induced cell scattering (Fig. 1A,C). When control cells were treated by HGF, they started to detach after 6 h of stimulation, and the cells gradually dispersed. By contrast, FilGAP-depleted cells started to detach after 2 h of stimulation with HGF. Live cell-imaging analysis showed that although control cells migrated at a constant speed after detachment, the migration speed of FilGAP-depleted cells increased during scattering (Fig. 1D; supplementary material Movies 1,2). Similar results were obtained using another FilGAP siRNA (data not shown). Forced expression of FilGAP in MDCKII cells suppressed cell scattering induced by HGF (Fig. 1E). MDCKII cells transfected with FilGAP adhered to each other and did not separate even at 18 h after addition of HGF.

Interestingly, the total amount of FilGAP protein expressed in MDCKII cells gradually decreased after the addition of HGF (Fig. 1F,G). The results suggest that FilGAP suppresses cell dissociation and migratory activity induced by HGF.

FilGAP regulates adherens junction integrity

FilGAP is a Rac-specific GAP and we first examined whether GAP activity of FilGAP is necessary for the suppression of HGF-induced scattering. MDCKII cells were transduced with lentiviral vectors expressing wild-type and a GAP-domain-deficient mutant FilGAP (ΔGAP FilGAP). Although wild-type FilGAP suppressed cell scattering after the stimulation of the cells with HGF for 18 h, ΔGAP FilGAP failed to suppress cell scattering induced by HGF (Fig. 2A,B). Therefore, Rac GAP activity of FilGAP might be necessary for the

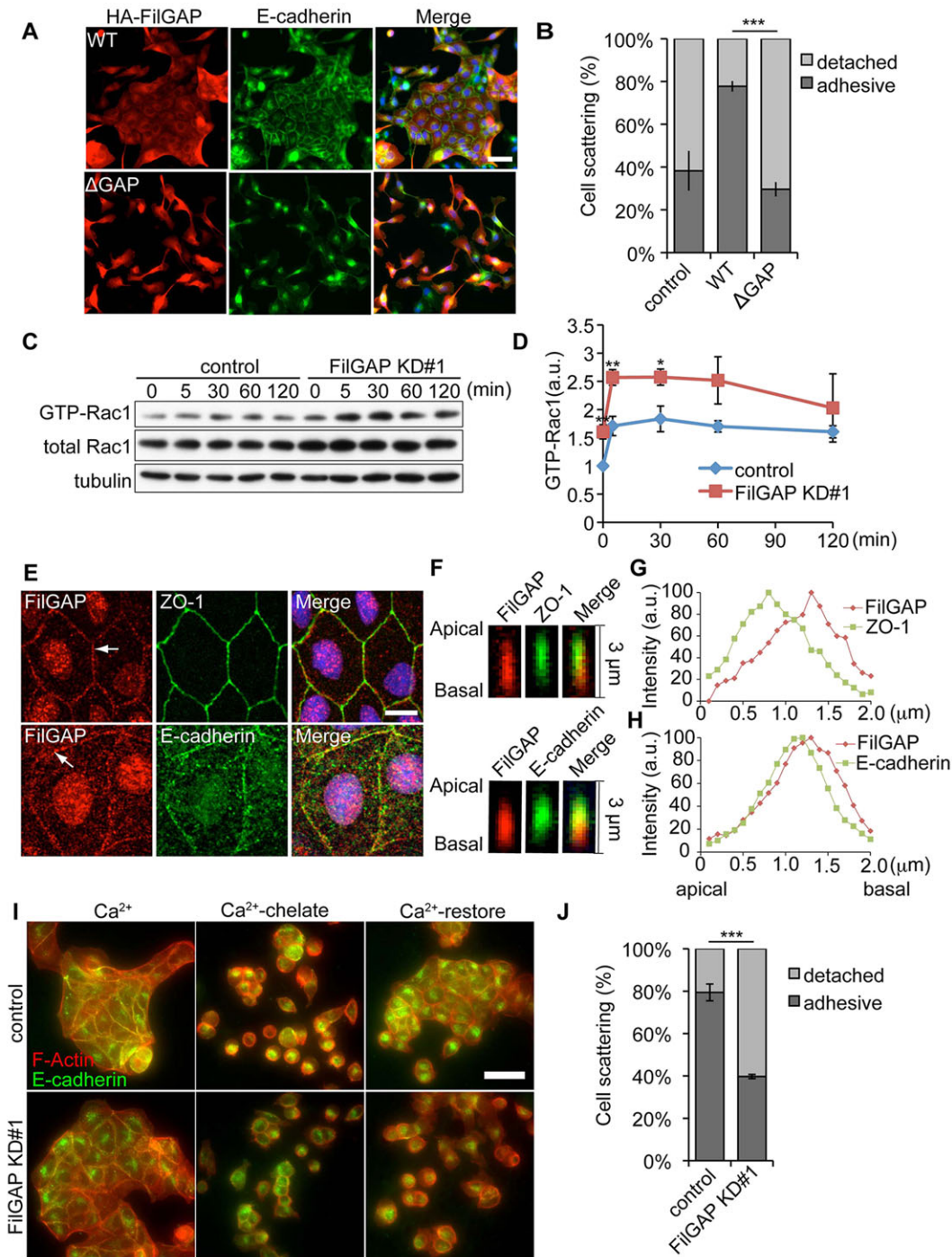


Fig. 2. FilGAP regulates E-cadherin-mediated cell–cell adhesion. (A) MDCKII cells transduced with lentiviral vectors encoding HA–FilGAP WT or HA–FilGAP lacking its GAP domain (Δ GAP) were fixed 18 h after the treatment with HGF (20 ng/ml) and stained with anti-HA (red) or anti-E-cadherin (green) antibodies. Cells were also stained with Hoechst 33258 to label nuclei. Scale bar: 50 μ m. (B) The percentages of scattering cells were calculated, and the data are expressed as the mean \pm s.e.m. ($n=3$). *** $P<0.001$ (Student's t -test). (C) FilGAP inactivates Rac during HGF-induced cell scattering. MDCKII cells were transfected with control or FilGAP siRNA for 2 days. Cell extracts were prepared after treatment with or without HGF (20 ng/ml) for the indicated time periods, and incubated with GST-RBD immobilized on glutathione–Sepharose beads. The amount of total Rac1 and GTP-Rac1 was detected by immunoblotting. (D) The percentages of GTP-Rac, treated as in C, were calculated, and the data are expressed as the mean \pm s.e.m. ($n=4$). * $P<0.05$, ** $P<0.01$ (Student's t -test). (E) MDCKII cells were permeabilized with 0.5% Triton X-100 for 5 min before fixation. Fixed cells were stained with polyclonal anti-FilGAP (red), and monoclonal anti-ZO1 (green) antibodies (upper panel) or anti-E-cadherin antibody (lower panel). Cells were also stained with Hoechst 33258 to label nuclei. Merged fluorescent images are shown. Scale bar: 10 μ m. (F) x - z views of the junction indicated by arrows in E showing the distribution of FilGAP (red) and ZO-1 (green), or FilGAP (red) and E-cadherin (green). Merged fluorescent images are shown. (G,H) Quantification of FilGAP and ZO-1 (G) or FilGAP and E-cadherin (H) at the junction as shown in E. (I) MDCKII cells were transfected with control or FilGAP siRNA for 2 days. Then the cells were treated with 4 mM EGTA for 30 min. Subsequently, the cells were treated with Ca²⁺-containing medium for 30 min. The cells were fixed and stained with anti-E-cadherin antibody for E-cadherin (green) and Alexa-Fluor-568-labeled phalloidin for F-actin (red). Scale bar: 50 μ m. (J) The percentages of scattering cells were calculated. The data are expressed as the mean \pm s.e.m. ($n=3$). *** $P<0.001$ (Student's t -test).

suppression of cell scattering induced by HGF. In accordance with this result, depletion of endogenous FilGAP by siRNA increased the amount of active Rac1 (GTP-Rac1) both under steady-state conditions and during HGF-induced cell scattering (Fig. 2C,D).

We next studied whether the effect of FilGAP on HGF-induced scattering is caused by the modulation of E-cadherin-dependent cell–cell adhesion. Endogenous FilGAP is localized at cell–cell junctions in MDCKII cells (Fig. 2E). The staining of FilGAP at cell–cell junctions is weak but specific because knockdown of endogenous FilGAP with siRNA eliminated the staining of FilGAP at cell–cell junctions (supplementary material Fig. S1A). FilGAP colocalized with E-cadherin at contacts but not with the tight junction marker ZO-1 (Fig. 2F–H). Therefore, FilGAP might localize at adherens junctions. These results suggest that FilGAP might stabilize adherens junctions through targeting E-cadherin at cell–cell adhesion.

E-cadherin mediates cell–cell adhesion by Ca^{2+} -dependent homophilic interactions. Using the Ca^{2+} switch model in MDCKII cells, we examined E-cadherin-mediated cell–cell adhesion. When cultured with a normal Ca^{2+} level, MDCKII cells formed E-cadherin-containing adhesions. By contrast, when cells were treated with EGTA, a Ca^{2+} chelator, these adhesions detached and dispersed (Fig. 2I,J). After restoration of Ca^{2+} , cell–cell adhesion was reconstructed in control cells, but FilGAP-depleted cells were unable to form cell–cell adhesions (Fig. 2I,J). These results suggest that FilGAP is required for E-cadherin-mediated cell–cell junction formation.

FilGAP regulates E-cadherin localization

We next examined whether FilGAP affects the localization of E-cadherin at adherens junctions to modulate cell–cell adhesion. MDCKII cells were transfected with FilGAP siRNA for 2 days. Then the cells were fixed and stained for filamentous actin (F-actin) and E-cadherin. In control MDCKII cells, E-cadherin localized at adherens junctions together with F-actin (Fig. 3A). Depletion of FilGAP by siRNA reduced the accumulation of E-cadherin at adherens junctions (Fig. 3A,C–E). Similar results were obtained using another FilGAP siRNA (data not shown). Conversely, forced expression of FilGAP induced the accumulation of E-cadherin at cell–cell junctions (Fig. 3B–E).

The reduction of E-cadherin accumulation at adherens junctions is more evident in MDCKII cells plated on Transwell membranes, which induce cell polarization (Fig. 3F). Depletion of FilGAP in cells plated on the membrane reduced E-cadherin intensity (Fig. 3G) and increased the cell area, probably owing to the reduced tension between the cells (Fig. 3H). To see whether the reduction in E-cadherin intensity is caused by the loss of E-cadherin expressed on the cell surface, surface-exposed E-cadherin was biotinylated and examined. As shown in Fig. 3I,J, depletion of FilGAP significantly reduced the surface expression of E-cadherin. Moreover, total amount of E-cadherin protein was also reduced by the depletion of FilGAP (Fig. 3K,L). Thus, knockdown of FilGAP might reduce both surface expression and total amount of E-cadherin.

FilGAP regulates E-cadherin downstream of ROCK

FilGAP is phosphorylated by ROCK, and phosphorylation stimulates its Rac GAP activity (Ohta et al., 2006). Moreover, E-cadherin-dependent cell–cell adhesion is dependent on Rho–ROCK signaling (Smutny et al., 2010). Therefore, we investigated whether FilGAP is located downstream of ROCK to modulate the formation of adherens junctions. Forced expression of full-length Myc-ROCK induced accumulation of E-cadherin at cell–cell junction (Fig. 4A,B). Depletion of endogenous FilGAP by siRNA reduced the

accumulation of E-cadherin at adherens junctions (Fig. 4A,B). Similar results were obtained using another FilGAP siRNA (data not shown). We further examined whether ROCK-mediated phosphorylation of FilGAP is required for accumulation of E-cadherin at adherens junctions. As shown in Fig. 4A and supplementary material Fig. S1B,C, depletion of FilGAP was rescued by overexpression of siRNA-resistant wild-type FilGAP but not a non-phosphorylatable FilGAP ST/A mutant. This demonstrates that ROCK stimulates accumulation of E-cadherin at cell–cell junction that might require ROCK-dependent phosphorylation of FilGAP.

Forced expression of wild-type FilGAP induced the accumulation of E-cadherin at adherens junctions. This accumulation was blocked by the treatment of the MDCKII cells with the ROCK-specific inhibitor Y27632 (Fig. 4C). However, overexpression of the phospho-mimic FilGAP ST/D mutant induced the localization of E-cadherin at adherens junctions in the presence of ROCK inhibitor. Thus, FilGAP might play a role in the regulation of localization of E-cadherin at adherens junctions downstream of ROCK.

We further examined whether phosphorylation of FilGAP by ROCK is involved in E-cadherin-dependent adhesion. MDCKII cells were transduced with lentiviral vectors expressing non-phosphorylatable (ST/A) or phospho-mimic (ST/D) HA–FilGAP mutants. We found that phospho-mimic FilGAP ST/D-expressing cells did not scatter after stimulation with HGF. By contrast, non-phosphorylatable FilGAP ST/A expressing cells dispersed even better than control cells after HGF treatment (Fig. 4D,E). Taken together, these data suggest that FilGAP might regulate E-cadherin localization downstream of ROCK.

FilGAP regulates E-cadherin through downregulation of Rac

FilGAP is a Rac-specific GAP and overexpression of FilGAP induced downregulation of Rac in MDCKII cells. Therefore, we expected that depletion of Rac1 would stimulate cell–cell adhesion induced by E-cadherin. MDCKII cells were transfected with Rac1 siRNA, and Rac1 was effectively depleted after 48 h (Fig. 5B). In Rac1-depleted cells, E-cadherin accumulated at cell–cell junctions (Fig. 5A,C). Knockdown of endogenous FilGAP reduced the accumulation of E-cadherin at adherens junctions but depletion of Rac1 rescued the loss of E-cadherin at adherens junctions induced by FilGAP siRNA (Fig. 5A,C). We also found that depletion of Rac1 suppressed HGF-induced cell scattering (Fig. 5D,E; supplementary material Movie 3). Similar results were obtained using another Rac1 siRNA (data not shown). Moreover, depletion of Rac1 blocked HGF-induced cell scattering stimulated by FilGAP siRNA (Fig. 5D,E; supplementary material Movie 4). These results suggest that FilGAP might induce accumulation of E-cadherin and block HGF-induced cell scattering through downregulation of Rac1.

We further examined whether FilGAP stabilizes adherens junctions through Rac1-mediated reorganization of the F-actin network. Forced expression of the constitutively activated Rac1 Q61L mutant induced a ruffle-like junctional F-actin network (Fig. 5F). A similar F-actin network was induced by depletion of FilGAP (Fig. 5F). The ruffle-like immature F-actin network at cell–cell junctions that was induced by knockdown of FilGAP was transformed into stress fibers by overexpression of the dominant-negative inhibitor Rac1 T17N mutant (Fig. 5F). Thus, downregulation of Rac1 by FilGAP might stabilize adherens junctions through re-organization of F-actin network.

DISCUSSION

In this study, we show that FilGAP mediates Rho–ROCK-dependent inactivation of Rac to stabilize adherens junctions. Rho

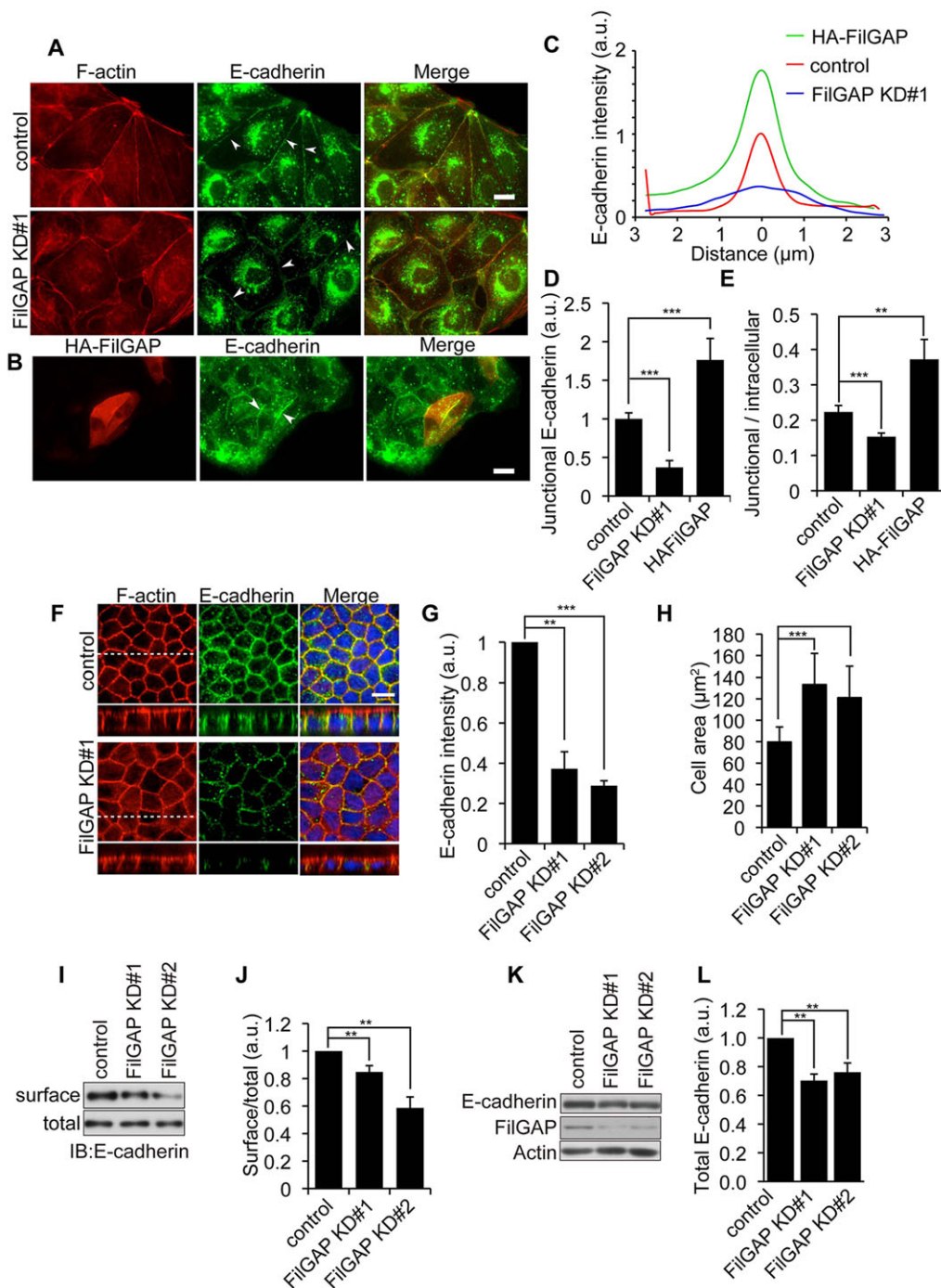


Fig. 3. FilGAP regulates the cellular localization of E-cadherin. (A) MDCKII cells were transfected with control or FilGAP siRNA for 2 days. Then the cells were fixed and stained with Alexa-Fluor-568-labeled phalloidin for F-actin (red) and anti-E-cadherin antibody (green). Merged fluorescent images are shown. Arrowheads indicate the localization of E-cadherin at cell contacts. Scale bar: 20 μm . (B) MDCKII cells were transiently transfected with HA-FilGAP. After 24 h, the cells were fixed and HA-FilGAP (red) and E-cadherin (green) were localized by staining the cells with anti-HA or anti-E-cadherin antibodies. Arrowheads indicate the localization of E-cadherin at cell contacts. Scale bar: 20 μm . (C) E-cadherin fluorescence intensities were quantified by line-scan analysis. (D) Junctional E-cadherin fluorescence intensities are shown ($n=3$). $***P<0.001$ (Student's *t*-test). (E) The ratio of junctional and intracellular E-cadherin fluorescence intensities are shown ($n=8-10$ cells). $***P<0.001$ (Student's *t*-test). (F) MDCKII cells were transfected with control or FilGAP siRNA and then cultured on filters for 4 days. Cells were then fixed and stained with Alexa-Fluor-568-labeled phalloidin for F-actin (red) and anti-E-cadherin antibody (green). Cells were also stained with Hoechst 33258 to label nuclei. Merged fluorescent images are shown. x-z views of the section indicated by the dotted lines are shown below. Scale bar: 5 μm . (G) Junctional E-cadherin fluorescence intensities are shown ($n=3$). $**P<0.05$, $***P<0.001$ (Student's *t*-test). (H) The cell area of MDCKII cells cultured on Transwell filters was calculated. Data are expressed as the mean \pm s.e.m. ($n=3$). $***P<0.001$ (Student's *t*-test). (I) MDCKII cells were transfected with control or FilGAP siRNAs and cultured on the filters for 4 days. Cells were surface-biotinylated at 0°C. Biotinylated proteins were recovered by streptavidin beads from cell extracts. E-cadherin levels were analyzed by immunoblotting. (J) Ratio of surface and total E-cadherin levels shown in I were calculated. The data are expressed as the mean \pm s.e.m. ($n=3$). $**P<0.05$ (Student's *t*-test). (K) MDCKII cells were transfected with control or FilGAP siRNAs and cultured for 2 days. E-cadherin levels were analyzed by immunoblotting. The amount of endogenous FilGAP is shown. Actin was used as a loading control. (L) E-cadherin levels shown in K were calculated and the data are expressed as the mean \pm s.e.m. ($n=4$).

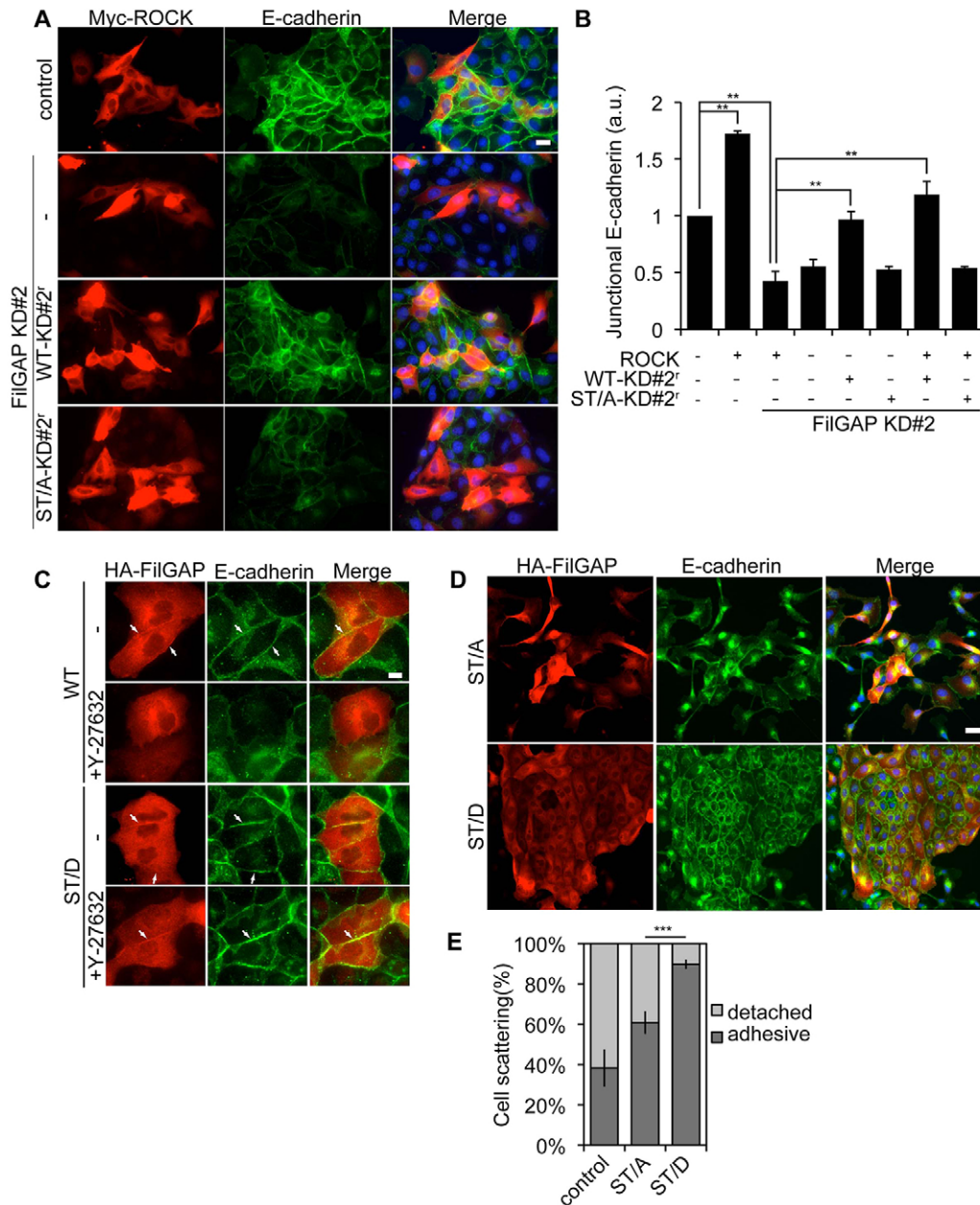


Fig. 4. FilGAP regulates E-cadherin localization downstream of ROCK. (A) MDCKII cells were transfected with control or FilGAP siRNA for 1 day. Then, the cells were transfected with indicated plasmids. After 24 h, the cells were fixed and stained with anti-E-cadherin antibody (green) and anti-Myc antibody (for Myc-ROCK, red). Cells were also stained with Hoechst 33258 to label nuclei. Merged fluorescent images are shown. Scale bar: 20 μ m. (B) Relative intensities of E-cadherin at cell junctions for the cells shown in A were calculated, and the data are expressed as the mean \pm s.e.m. ($n=3$). $**P<0.05$ (Student's t -test). (C) MDCKII cells were transfected with HA-FilGAP WT or phospho-mimic (ST/D) HA-FilGAP mutant for 2 days. Then the cells were fixed after the treatment with or without Y27632 (10 μ M), and HA-FilGAP (red) or E-cadherin (green) was localized by staining the cells with anti-FilGAP or anti-E-cadherin antibodies. Merged fluorescent images are shown. Scale bar: 100 μ m. Arrows indicate the cell-cell junctions. (D) MDCKII cells were transduced with lentiviral vectors expressing non-phosphorylatable (ST/A) or phospho-mimic (ST/D) HA-FilGAP mutants. The cells were fixed 18 h after the treatment of the cells with HGF (20 ng/ml), and HA-FilGAP (red) or E-cadherin (green) was localized by staining the cells with anti-FilGAP or anti-E-cadherin antibodies. Cells were also stained with Hoechst 33258 to label nuclei. Merged fluorescence images are shown. Scale bar: 100 μ m. (E) The percentages of scattering cells shown in D were calculated. Data are expressed as the mean \pm s.e.m. ($n=3$). $***P<0.001$ (Student's t -test).

GTPases are required for the formation and maintenance of adherens junctions. Rac is activated as an early response to E-cadherin-mediated cell-cell adhesion. Rac activity is then replaced by Rho and Rho, which is required for expansion and stabilization of adherens junctions (Noren et al., 2003; Yamada and Nelson, 2007). Therefore, the balance in the activity of Rac and Rho at adherens junctions should be spatiotemporally determined by

Rho GTPase regulators (Ngok et al., 2014; Niessen et al., 2011). Our present study suggests that FilGAP is involved in the maintenance of the 'Rho zone' at adherens junctions.

The integrity of adherens junctions is regulated by Rho-ROCK signaling (Shewan et al., 2005). Myosin IIA is a major downstream effector of the Rho-ROCK pathway (Smutny et al., 2010). Phosphorylation of myosin IIA by ROCK stabilized actin

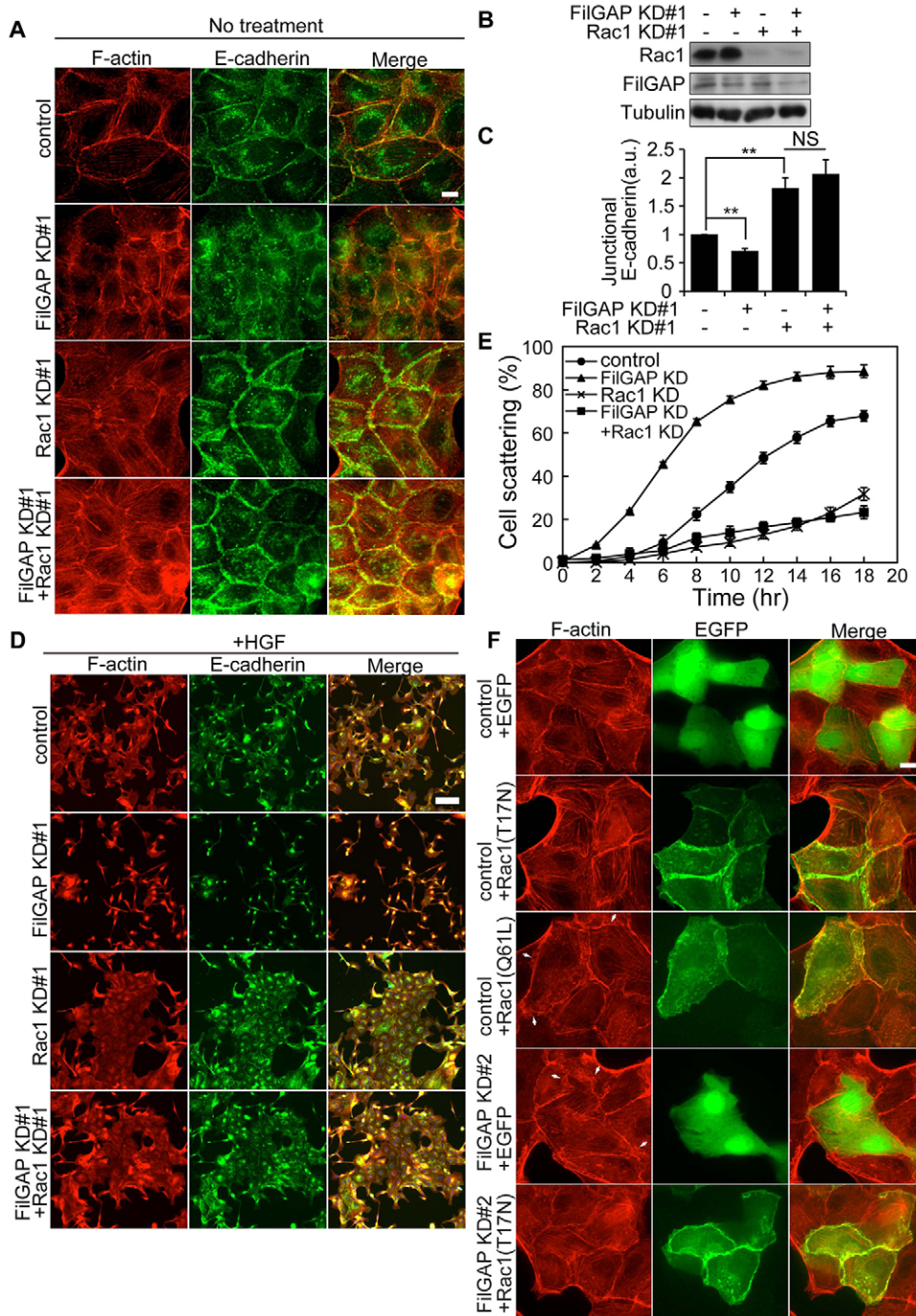


Fig. 5. FilGAP regulates E-cadherin localization and HGF-induced cell scattering upstream Rac1. (A) MDCKII cells were transfected with control, FilGAP or Rac1 siRNAs for 2 days. Then the cells were fixed and F-actin (red) or E-cadherin (green) was localized by staining the cells with Alexa-Fluor-568-labeled phalloidin for F-actin and anti-E-cadherin. Scale bar: 10 μ m. (B) Immunoblot showing that Rac1 and FilGAP are depleted after 2 days of siRNA treatment in MDCKII cells. Tubulin was used as a loading control. (C) Junctional E-cadherin fluorescence intensities are shown. E-cadherin fluorescence intensities were quantified by line-scan analysis. $**P < 0.01$ (Student's *t*-test). (D) MDCKII cells were transfected with control, FilGAP or Rac1 siRNAs for 2 days. The cells were fixed 18 h after the treatment with HGF (20 ng/ml) and F-actin (red) or E-cadherin (green) was localized by staining the cells with Alexa-Fluor-568-labeled phalloidin for F-actin and anti-E-cadherin antibody. Scale bar: 100 μ m. (E) The percentages of scattering cells were calculated, and the data are expressed as the mean \pm s.e.m. ($n=3$). (F) MDCKII cells were transfected with control or FilGAP siRNA for 1 day. Then, the cells were transfected with EGFP, EGFP-Rac1(T17N) or EGFP-Rac1(Q61L). After 24 h, the cells were fixed and stained with Alexa-Fluor-568-labeled phalloidin for F-actin. Arrows indicate ruffle-like structures. Scale bar: 10 μ m.

cytoskeleton at adherens junctions. Our present study suggests that ROCK is not only involved in the activation of myosin II but is also required for the suppression of Rac through activation of FilGAP. First, depletion of endogenous FilGAP blocked the accumulation of E-cadherin at adherens junctions induced by overexpression of ROCK (Fig. 5A). Moreover, the accumulation of E-cadherin at adherens junctions was recovered upon the expression of siRNA-resistant wild-type FilGAP but not by the expression of the non-phosphorylatable FilGAP ST/A mutant. Second, forced expression of the phospho-mimic FilGAP ST/D mutant induced accumulation of E-cadherin at adherens junctions in the presence of the ROCK-specific inhibitor Y27632. Taken together, our study suggests that stabilization of E-cadherin at adherens junctions might require

activation of FilGAP downstream of ROCK. A previous study has demonstrated that the centralspindlin complex associates with α -catenin and supports Rho activation through recruitment of the Rho GEF ECT2 and suppression of Rac through modulating its Rac GAP activity (Ratheesh et al., 2012). Once this pathway is activated, FilGAP could function downstream of Rho-ROCK to maintain Rho activation. Although FilGAP is colocalized with E-cadherin at adherens junctions, we could not demonstrate the direct association of FilGAP with E-cadherin and/or α -catenin. Further work is necessary to determine how FilGAP is targeted to adherens junctions.

It is unclear how FilGAP stabilizes E-cadherin at adherens junctions. However, our study suggests that inactivation of Rac by FilGAP might play a role in targeting of E-cadherin at adherens

junctions. First, the Rac GAP activity of FilGAP is required for stabilization of cell–cell adhesions (Fig. 2A). Second, ROCK-mediated activation of FilGAP seems to be necessary for E-cadherin accumulation at adherens junctions (Fig. 4). Finally, knockdown of endogenous FilGAP reduced the accumulation of E-cadherin at adherens junctions but depletion of endogenous Rac1 rescued the localization of E-cadherin at adherens junctions in the presence of FilGAP siRNA (Fig. 5). A previous study has shown that depletion of TEM4, a Rho GEF, impairs cell–cell junction formation in MDCK cells and reduces the amount of activated RhoA (Ngok et al., 2013). Thus, the balance in the activity of Rac and Rho as a result of activation of Rho or inactivation of Rac might be necessary for the maintenance of adherens junctions.

It remains to be determined how inactivation of Rac1 induces accumulation of E-cadherin at adherens junctions. Our results showed that the F-actin network at adherens junctions is affected by Rac1 activity. Both overexpression of dominant-negative Rac1 (Rac1 T17N) and knockdown of endogenous Rac1 induced the formation of a dense cortical F-actin network at adherens junctions, which was accompanied by the accumulation of E-cadherin at adherens junctions (Fig. 5). Therefore, inactivation of Rac1 by FilGAP might stabilize the F-actin network and maintains E-cadherin localization at adherens junctions. Rac and Rho might antagonize each other at adherens junctions, and inactivation of Rac1 at adherens junctions might induce activation of Rho, which would in turn stabilize the F-actin network (Ratheesh et al., 2012).

We showed that depletion of FilGAP reduced the total amount as well as cell surface expression of E-cadherin (Fig. 3I–L). The mechanism of regulation is unknown; however, FilGAP could stabilize E-cadherin at the cell surface through regulation of endocytosis of E-cadherin. Previous studies have shown that Rac could inhibit or activate E-cadherin endocytosis (Akhtar and Hotchin, 2001; Izumi et al., 2004; Lozano et al., 2003). A similar mechanism might be responsible for the reduced E-cadherin localization at adherens junctions upon knockdown of FilGAP.

HGF stimulates disruption of cell–cell junctions and enhances cell migration and scattering in a number of epithelial cell lines including MDCK cells. Our study suggests that FilGAP might suppress cell scattering induced by HGF. First, depletion of endogenous FilGAP in MDCKII cells stimulated the detachment of cells after the addition of HGF. Moreover, the speed of cell migration increased during HGF-induced scattering. Second, forced expression of FilGAP suppressed detachment of cells after the addition of HGF. Third, the total amount of FilGAP protein decreased after the addition of HGF. This might facilitate the disassembly of adherens junctions stabilized by FilGAP. ARHGAP12 has been identified as a Rac GAP that is associated at adherens junctions and is also transcriptionally downregulated by HGF (Gentile et al., 2008; Matsuda et al., 2008). Moreover, depletion of ARHGAP12 stimulates HGF scattering (Gentile et al., 2008). Therefore, the biological function of ARHGAP12 seems to be similar to that of FilGAP. However, it is unclear how the activity of ARHGAP12 is regulated. Further study is required to understand the relations between FilGAP and ARHGAP12.

It remains to be determined how FilGAP suppresses cell scattering, but downregulation of Rac seems to be involved not only in the stabilization of adherens junctions but also the suppression of HGF-mediated scattering. We showed that depletion of Rac1 blocked HGF-induced cell scattering (Fig. 5). Knockdown of FilGAP failed to stimulate HGF-induced cell scattering in the absence of endogenous Rac1 (Fig. 5). In agreement with this result, previous studies have shown that activation of Rac1 and its effector PAK1 are involved in

HGF-induced cell scattering (Bright et al., 2009; Ridley et al., 1995). Moreover, depletion of Numb, an endocytic adaptor protein, stimulates cell scattering induced by HGF, which is inhibited by the Rac1 inhibitor NSC23766 (Lau and McGlade, 2011). Numb depletion in epithelial cells causes increased Rac1 activation, which correlates with destabilized cell–cell junctions and potentiation of HGF-induced cell dispersal. Our study also showed that depletion of FilGAP induced activation of Rac1 (Fig. 2).

Malignant tumor cells invade through tissue extracellular matrix by using two interconvertible modes of cell motility referred to as mesenchymal and amoeboid migration (Friedl and Alexander, 2011; Sanz-Moreno and Marshall, 2010). Our previous study showed that FilGAP contributes to the regulation of mesenchymal to amoeboid transition (Saito et al., 2012). Forced expression of FilGAP induced membrane blebbing and a rounded amoeboid morphology that requires Rho–ROCK-dependent phosphorylation of FilGAP (Ohta et al., 2006). Recent studies have shown that hyperactivation of Met induced membrane blebbing, which leads to amoeboid cell motility and invasion (Laser-Azogui et al., 2014). Moreover, transformation of MDCK cells with moloney sarcoma virus cells induced membrane blebbing, which is dependent on Rho–ROCK signaling and requires autocrine c-Met activation (Jia et al., 2006). FilGAP could be involved in the HGF and Met signaling in those invasive cancer cells.

We have shown previously that FilGAP functions downstream of Arf6, and that Arf6 stimulates FilGAP-dependent suppression of Rac (Kawaguchi et al., 2014). Arf6 has been shown to suppress Rac by inhibiting Tiam-1 Rac GEF at adherens junctions (Palacios et al., 2002). It is therefore possible Arf6 might utilize FilGAP to modulate the integrity of adherens junctions.

In summary, our present study demonstrates that FilGAP might function to maintain adherens junction integrity through inactivation of Rac downstream of Rho–ROCK signaling. FilGAP might be crucially involved as a Rho GTPase regulator to determine the balance of Rac and Rho activities at adherens junctions.

MATERIALS AND METHODS

Plasmids and siRNA

The HA-tagged FilGAP (wild-type, ST/A, ST/D and Δ GAP) constructs in pCMV5 vector were as described previously (Ohta et al., 2006). EGFP-C1-Rac1(T17N) was generated by PCR. pcDNA3-EGFP-Rac1 Q61L was purchased from Addgene (plasmid ID 12981, Cambridge, MA). CSII-EF-MCS–HA-FilGAP [wild type (WT), ST/A ST/D and Δ GAP] vectors were generated by PCR. The FilGAP siRNA KD#2-resistant construct (KD#2r) was generated by introducing point mutations at nucleotide positions 1980, 1986, 1992 and 1995 of the FilGAP coding sequence using the QuikChange site-directed mutagenesis kit. siRNA oligonucleotide duplexes targeting FilGAP and Rac1 were purchased from Invitrogen (Carlsbad, CA). The targeting sequences were as follows: FilGAP, KD#1 5'-AAGAUAGAGU-AUGAGUCCAGGAUAA-3' (nt 1975–1999) and KD#2 5'-CAGUGAUG-AUUAGCAAACAUGAUUG-3' (nt 956–980); Rac1, KD#1 5'-UUUAC-CUACAGCUCGUCUCCACC-3' (nt 24–48) and KD#2 5'-AGCAA-AUUAAAGAACACAUCUGUUUG-3' (nt 220–244).

Antibodies and reagents

Mouse anti-HA (12CA5), and anti- α -tubulin monoclonal antibodies were purchased from Sigma. Rabbit anti-Myc antibody was purchased from MBL (Nagoya, Japan). Mouse anti-E-cadherin antibody was purchased from BD biosciences (Bedford, MA). Mouse anti-Rac1 monoclonal antibody was purchased from Millipore (Billerica, MA). Rabbit anti-FilGAP polyclonal antibody was prepared as described previously (Ohta et al., 2006). Mouse anti-ZO-1 antibody and secondary antibodies conjugated to Alexa Fluor 488 or 568, and Alexa-Fluor-568–phalloidin were purchased from Invitrogen. HGF was from Millipore.

Cell culture and transfection

MDCKII cells were cultured in Dulbecco's modified Eagle's medium (DMEM, Sigma-Aldrich, St Louis, MO) supplemented with 10% (v/v) fetal bovine serum (FBS) and 50 U/ml penicillin-streptomycin at 37°C under 5% CO₂. Cells were transfected with plasmid DNA for 24 h or FilGAP siRNA for 48–72 h using Lipofectamine 2000 and Lipofectamine RNAiMax (Invitrogen) according to the manufacturer's instructions. To disrupt E-cadherin-mediated cell–cell contacts, serum-starved MDCKII cells were incubated with medium containing 4 mM EGTA at 37°C for 30 min. Then, the cells were incubated with DMEM containing a normal Ca²⁺ concentration to induce cell–cell contacts for indicated times at 37°C.

Microscopy

For immunofluorescence staining, cells were washed twice with PBS and fixed with 3.7% (v/v) formaldehyde for 10 min. Fixed cells were permeabilized with 0.5% Triton X-100 in PBS for 10 min and stained with Alexa-Fluor-568–phalloidin for F-actin or immunostained with primary antibodies. Cells were then washed and incubated with Alexa-Fluor-dye-labeled secondary antibodies (Invitrogen). After washing with PBS, cells were observed under an Olympus IX81 fluorescence microscope (Olympus, Tokyo, Japan). Images were acquired by a charge-coupled device (CCD) camera (ORCA-ER; Hamamatsu Photonics, Hamamatsu, Japan) or an EMCCD camera (iXon3; Andor, South Windsor, CT) and MetaMorph software (Molecular Devices, Sunnyvale, CA). Confocal images were obtained using Olympus DSU (Disk scanning unit)-IX81 with a 100× objective. Time-lapse DIC images were recorded at 12 min intervals for 24 h.

RhoGAP assay

MDCK cells treated with control or FilGAP siRNA were cultured for 48 h. After incubation with or without 20 ng/ml HGF for 4 h, cells were directly lysed in RIPA buffer [20 mM Tris-HCl pH 7.5, 500 mM NaCl, 10 mM MgCl₂, 1% Triton X-100, 0.5% sodium deoxycholate, 0.1% SDS and protease inhibitor cocktails (Sigma)] at 4°C. The cell lysates were pre-cleared and samples of supernatants fluids were withdrawn for the determination of total Rac protein, and the remaining supernatants were incubated with 20 μg of GST-PAK-CRIB protein in the presence of glutathione–Sephareose beads (GE Healthcare). The beads were washed and the level of GTP-bound Rac1 was determined by immunoblotting using anti-Rac1 antibody.

Cell surface biotinylation

Cell surface biotinylation was performed as described previously (Fujita et al., 2002). Briefly, MDCK cells grown on filters (cell culture inserts, Thermo Scientific) were incubated with 0.5 mg/ml sulfo-NHS-SS-biotin (Thermo Scientific) for 1 h at 0°C, which was applied to both apical and basal sides of the filter, followed by washing by blocking reagent (50 mM NH₄Cl, 1 mM MgCl₂, 0.1 mM CaCl₂). Cells were lysed in RIPA buffer and cell extracts were incubated with streptavidin beads (Sigma) to collect bound biotinylated proteins. Samples were then analyzed by SDS-PAGE and immunoblotting.

Statistical analysis

The statistical significance was accessed by two-tailed unpaired Student's *t*-test. Differences were considered to be statistically significant at *P* < 0.05. Error bars (s.e.m.) and *P* values were determined from results of at least three experiments.

Competing interests

The authors declare no competing or financial interests.

Author contributions

S.N., K.T. and Y.O. designed the study, analyzed the data and wrote the paper. S.N., K.T. and T.Z. performed the experiments.

Funding

This work was supported by Grants-in-Aid for Scientific Research from the Japan Society for the Promotion of Science and the Ministry of Education, Culture, Sports,

Science, and Technology of Japan, Grant for All Kitasato Project Study, and Kitasato University Research Grant for Young Researchers.

Supplementary material

Supplementary material available online at <http://jcs.biologists.org/lookup/suppl/doi:10.1242/jcs.160192/-/DC1>

References

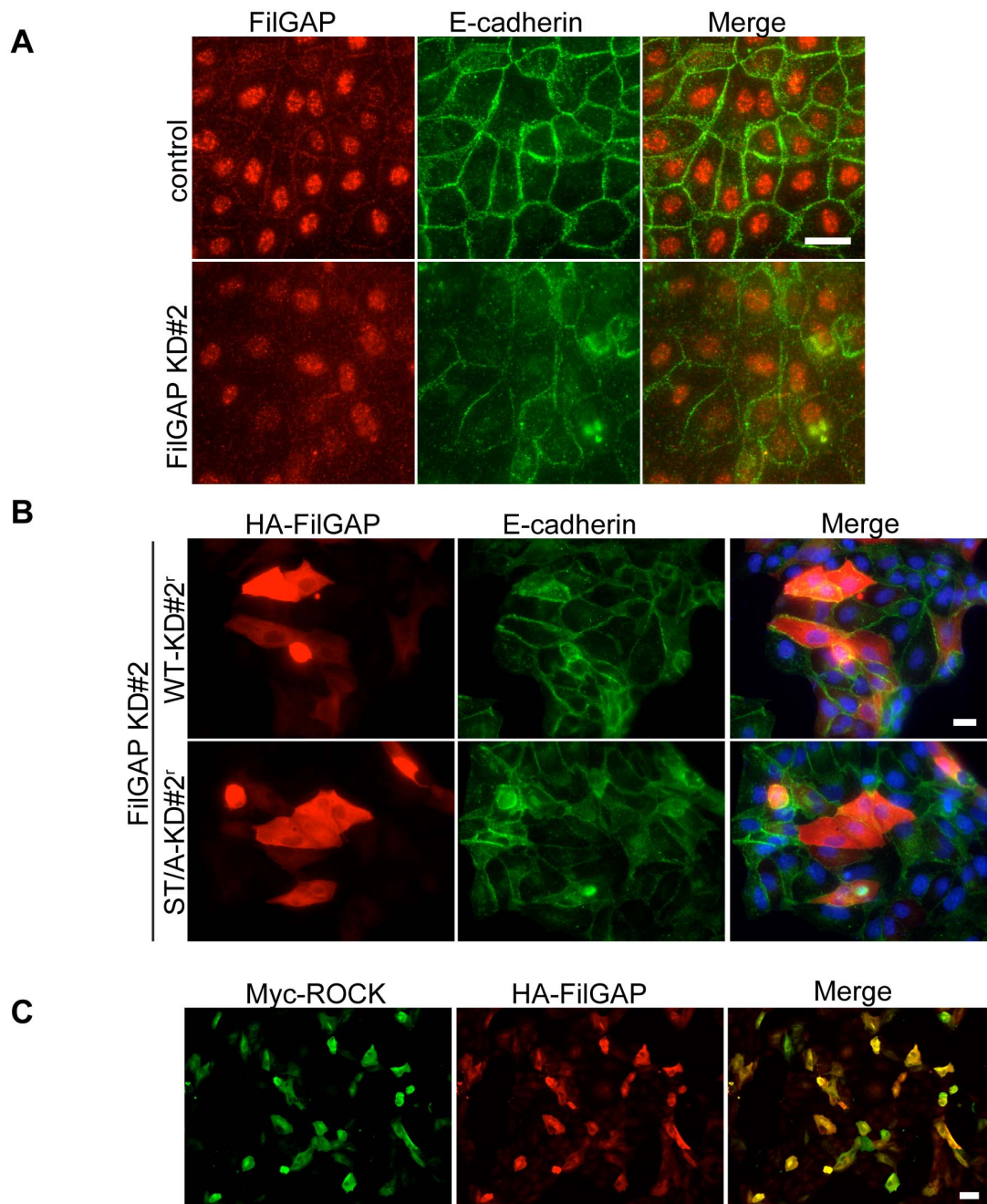
- Akhtar, N. and Hotchin, N. A. (2001). RAC1 regulates adherens junctions through endocytosis of E-cadherin. *Mol. Biol. Cell* **12**, 847–862.
- Bos, J. L., Rehmann, H. and Wittinghofer, A. (2007). GEFs and GAPs: critical elements in the control of small G proteins. *Cell* **129**, 865–877.
- Brieher, W. M. and Yap, A. S. (2013). Cadherin junctions and their cytoskeleton(s). *Curr. Opin. Cell Biol.* **25**, 39–46.
- Bright, M. D., Garner, A. P. and Ridley, A. J. (2009). PAK1 and PAK2 have different roles in HGF-induced morphological responses. *Cell. Signal.* **21**, 1738–1747.
- Ehrlich, J. S., Hansen, M. D. and Nelson, W. J. (2002). Spatio-temporal regulation of Rac1 localization and lamellipodia dynamics during epithelial cell–cell adhesion. *Dev. Cell* **3**, 259–270.
- Friedl, P. and Alexander, S. (2011). Cancer invasion and the microenvironment: plasticity and reciprocity. *Cell* **147**, 992–1009.
- Fujita, Y., Krause, G., Scheffner, M., Zechner, D., Leddy, H. E., Behrens, J., Sommer, T. and Birchmeier, W. (2002). Hakai, a c-Cbl-like protein, ubiquitinates and induces endocytosis of the E-cadherin complex. *Nat. Cell Biol.* **4**, 222–231.
- Gentile, A., D'Alessandro, L., Lazzari, L., Martinoglio, B., Bertotti, A., Mira, A., Lanzetti, L., Comoglio, P. M. and Medico, E. (2008). Met-driven invasive growth involves transcriptional regulation of Arhgap12. *Oncogene* **27**, 5590–5598.
- Gravel, C. R., Tolbert, D. and Vande Woude, G. F. (2013). MET: a critical player in tumorigenesis and therapeutic target. *Cold Spring Harb. Perspect. Biol.* **5**, a009209.
- Green, K. J., Getsios, S., Troyanovsky, S. and Godsel, L. M. (2010). Intercellular junction assembly, dynamics, and homeostasis. *Cold Spring Harb. Perspect. Biol.* **2**, a000125.
- Guilluy, C., Garcia-Mata, R. and Burridge, K. (2011). Rho protein crosstalk: another social network? *Trends Cell Biol.* **21**, 718–726.
- Heasman, S. J. and Ridley, A. J. (2008). Mammalian Rho GTPases: new insights into their functions from in vivo studies. *Nat. Rev. Mol. Cell Biol.* **9**, 690–701.
- Izumi, G., Sakisaka, T., Baba, T., Tanaka, S., Morimoto, K. and Takai, Y. (2004). Endocytosis of E-cadherin regulated by Rac and Cdc42 small G proteins through IQGAP1 and actin filaments. *J. Cell Biol.* **166**, 237–248.
- Jaffe, A. B. and Hall, A. (2005). Rho GTPases: biochemistry and biology. *Annu. Rev. Cell Dev. Biol.* **21**, 247–269.
- Jia, Z., Vadnais, J., Lu, M. L., Noël, J. and Nabi, I. R. (2006). Rho/ROCK-dependent pseudopodial protrusion and cellular blebbing are regulated by p38 MAPK in tumour cells exhibiting autocrine c-Met activation. *Biol. Cell* **98**, 337–351.
- Kawaguchi, K., Saito, K., Asami, H. and Ohta, Y. (2014). ADP ribosylation factor 6 (Arf6) acts through FilGAP protein to down-regulate Rac protein and regulates plasma membrane blebbing. *J. Biol. Chem.* **289**, 9675–9682.
- Kodama, A., Matozaki, T., Fukuhara, A., Kikyo, M., Ichihashi, M. and Takai, Y. (2000). Involvement of an SHP-2-Rho small G protein pathway in hepatocyte growth factor/scatter factor-induced cell scattering. *Mol. Biol. Cell* **11**, 2565–2575.
- Kovacs, E. M., Ali, R. G., McCormack, A. J. and Yap, A. S. (2002). E-cadherin homophilic ligation directly signals through Rac and phosphatidylinositol 3-kinase to regulate adhesive contacts. *J. Biol. Chem.* **277**, 6708–6718.
- Laser-Azogui, A., Diamant-Levi, T., Israeli, S., Roytman, Y. and Tsarfaty, I. (2014). Met-induced membrane blebbing leads to amoeboid cell motility and invasion. *Oncogene* **33**, 1788–1798.
- Lau, K. M. and McGlade, C. J. (2011). Numb is a negative regulator of HGF dependent cell scattering and Rac1 activation. *Exp. Cell Res.* **317**, 539–551.
- Lozano, E., Betson, M. and Braga, V. M. (2003). Tumor progression: small GTPases and loss of cell–cell adhesion. *BioEssays* **25**, 452–463.
- Matsuda, M., Kobayashi, Y., Masuda, S., Adachi, M., Watanabe, T., Yamashita, J. K., Nishi, E., Tsukita, S. and Furuse, M. (2008). Identification of adherens junction-associated GTPase activating proteins by the fluorescence localization-based expression cloning. *Exp. Cell Res.* **314**, 939–949.
- McCormack, J., Welsh, N. J. and Braga, V. M. (2013). Cycling around cell–cell adhesion with Rho GTPase regulators. *J. Cell Sci.* **126**, 379–391.
- Nakamura, F. (2013). FilGAP and its close relatives: a mediator of Rho-Rac antagonism that regulates cell morphology and migration. *Biochem. J.* **453**, 17–25.
- Ngok, S. P., Geyer, R., Kourtidis, A., Mitin, N., Feathers, R., Der, C. and Anastasiadis, P. Z. (2013). TEM4 is a junctional Rho GEF required for cell–cell adhesion, monolayer integrity and barrier function. *J. Cell Sci.* **126**, 3271–3277.
- Ngok, S. P., Lin, W. H. and Anastasiadis, P. Z. (2014). Establishment of epithelial polarity – GEF who's minding the GAP? *J. Cell Sci.* **127**, 3205–3215.
- Niessen, C. M., Leckband, D. and Yap, A. S. (2011). Tissue organization by cadherin adhesion molecules: dynamic molecular and cellular mechanisms of morphogenetic regulation. *Physiol. Rev.* **91**, 691–731.
- Noren, N. K., Niessen, C. M., Gumbiner, B. M. and Burridge, K. (2001). Cadherin engagement regulates Rho family GTPases. *J. Biol. Chem.* **276**, 33305–33308.

- Noren, N. K., Arthur, W. T. and Burridge, K.** (2003). Cadherin engagement inhibits RhoA via p190RhoGAP. *J. Biol. Chem.* **278**, 13615-13618.
- Ohta, Y., Hartwig, J. H. and Stossel, T. P.** (2006). FilGAP, a Rho- and ROCK-regulated GAP for Rac binds filamin A to control actin remodelling. *Nat. Cell Biol.* **8**, 803-814.
- Palacios, F., Schweitzer, J. K., Boshans, R. L. and D'Souza-Schorey, C.** (2002). ARF6-GTP recruits Nm23-H1 to facilitate dynamin-mediated endocytosis during adherens junctions disassembly. *Nat. Cell Biol.* **4**, 929-936.
- Parsons, J. T., Horwitz, A. R. and Schwartz, M. A.** (2010). Cell adhesion: integrating cytoskeletal dynamics and cellular tension. *Nat. Rev. Mol. Cell Biol.* **11**, 633-643.
- Ratheesh, A., Gomez, G. A., Priya, R., Verma, S., Kovacs, E. M., Jiang, K., Brown, N. H., Akhmanova, A., Stehbens, S. J. and Yap, A. S.** (2012). Centralspindlin and α -catenin regulate Rho signalling at the epithelial zonula adherens. *Nat. Cell Biol.* **14**, 818-828.
- Ridley, A. J., Comoglio, P. M. and Hall, A.** (1995). Regulation of scatter factor/hepatocyte growth factor responses by Ras, Rac, and Rho in MDCK cells. *Mol. Cell Biol.* **15**, 1110-1122.
- Saito, K., Ozawa, Y., Hibino, K. and Ohta, Y.** (2012). FilGAP, a Rho/Rho-associated protein kinase-regulated GTPase-activating protein for Rac, controls tumor cell migration. *Mol. Biol. Cell* **23**, 4739-4750.
- Sanz-Moreno, V. and Marshall, C. J.** (2010). The plasticity of cytoskeletal dynamics underlying neoplastic cell migration. *Curr. Opin. Cell Biol.* **22**, 690-696.
- Shewan, A. M., Maddugoda, M., Kraemer, A., Stehbens, S. J., Verma, S., Kovacs, E. M. and Yap, A. S.** (2005). Myosin 2 is a key Rho kinase target necessary for the local concentration of E-cadherin at cell-cell contacts. *Mol. Biol. Cell* **16**, 4531-4542.
- Smutny, M., Cox, H. L., Leerberg, J. M., Kovacs, E. M., Conti, M. A., Ferguson, C., Hamilton, N. A., Parton, R. G., Adelstein, R. S. and Yap, A. S.** (2010). Myosin II isoforms identify distinct functional modules that support integrity of the epithelial zonula adherens. *Nat. Cell Biol.* **12**, 696-702.
- Yamada, S. and Nelson, W. J.** (2007). Localized zones of Rho and Rac activities drive initiation and expansion of epithelial cell-cell adhesion. *J. Cell Biol.* **178**, 517-527.

Supplementary Figure

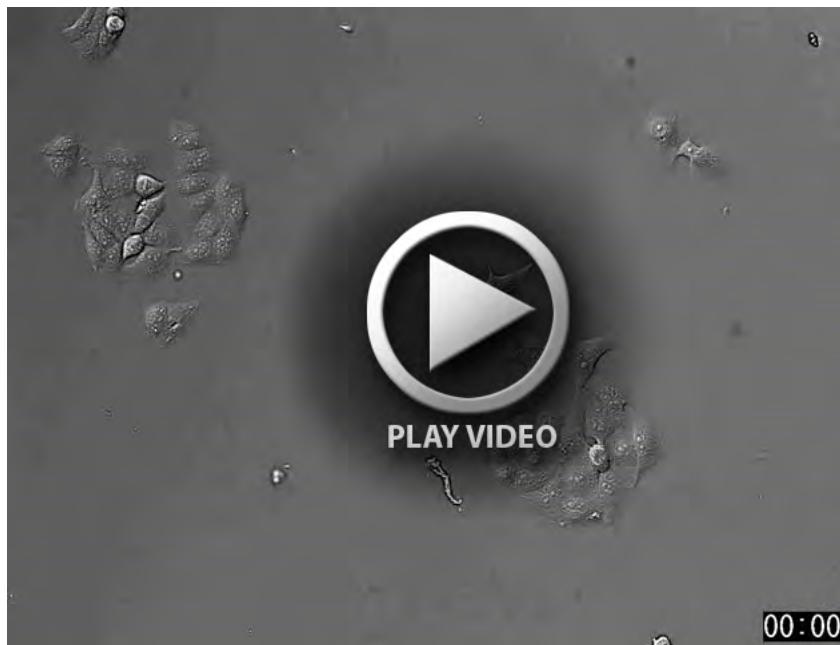
Fig. S1 Localization of endogenous FilGAP in MDCK II cells. (A) MDCK II cells were transfected with control or *FilGAP* siRNA for 72 hr. Then the cells were permeabilized by 0.5 % TritonX-100 before fixation. Permeabilized cells were fixed and stained with anti-FilGAP (red) or anti-E-cadherin (green) antibodies. Merged fluorescent images are shown. Scale bar, 20 μ m. (B) MDCK II cells were transfected with FilGAP siRNA for 1 d. Then, the cells were transfected with RNAi resistant FilGAP(WT-KD#2^r or ST/A-KD#2^r). After 24 hr, the cells were fixed and stained with anti-E-cadherin antibody for E-cadherin (green) and anti-Myc antibody for Myc-ROCK (red). Cells were also labeled with hoechst 33258 for nuclei. Merged fluorescent images were shown. Scale bar, 20 μ m. (C) MDCK II cells were transfected with Myc-ROCK and HA-FilGAP (WT-KD#2^r). After 24 hr, the cells were fixed and stained with anti-Myc antibody for Myc-ROCK (green) and anti-HA antibody for HA-FilGAP. Merged fluorescent images were shown. Most of cells express both Myc-ROCK and HA-FilGAP (>95%). Scale bar, 50 μ m.

Fig. S1





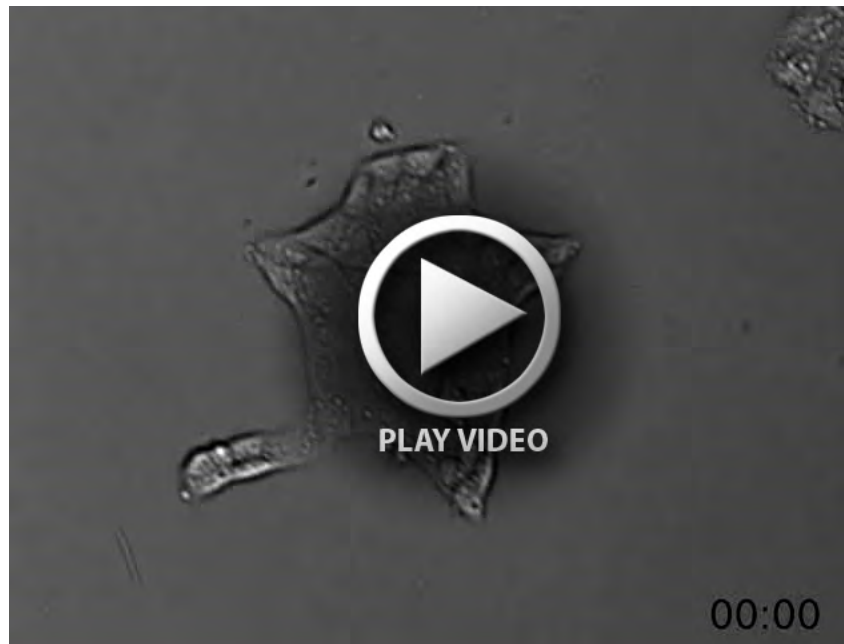
Movie 1. HGF-induced cell scattering (control MDCK II cells)



Movie 2. HGF-induced cell scattering (FilGAP-depleted MDCK II cells)



Movie 3. HGF-induced cell scattering (Rac1-depleted MDCK II cells)



Movie 4. HGF-induced cell scattering (FilGAP- and Rac1-depleted MDCK II cells)